Supplementary Information

Influences of Fluid and System Design Parameters on Hydrodynamically Driven Low Gradient Magnetic Separation of Magnetic Nanoparticles

Yee Win Tan[a], *Priscilla Fong Ern Gunn*[a], *Wei Ming Ng*[b], *Sim Siong Leong**[c], *Pey Yi Toh*[a], *Juan Camacho*[d], *Jordi Faraudo*[e], *JitKang Lim*[b]

[a]Department of Petrochemical Engineering, Faculty of Engineering and Green Technology, Universiti Tunku Abdul Rahman, Kampar 31900, Perak, Malaysia.

[b]School of Chemical Engineering, Universiti Sains Malaysia, Nibong Tebal, Penang 14300, Malaysia.

[c]Department of Industrial Engineering, Faculty of Engineering and Green Technology, Universiti Tunku Abdul Rahman, Kampar 31900, Perak, Malaysia.

[d]Departament de Física, Facultat de Ciències, Universitat Autònoma de Barcelona, E-08193 Bellaterra, Spain

[e]Institut de Ciència de Materials de Barcelona (ICMAB-CSIC), C/ dels Til.lers s/n, Campus UAB, E-08193 Bellaterra, Spain.

*****To whom correspondence should be addressed:

Sim Siong Leong
Department of Industrial Engineering,
Faculty of Engineering and Green Technology,
Universiti Tunku Abdul Rahman,
Kampar 31900, Perak, Malaysia.
E-mail: leongss@utar.edu.my; leongsimsiong@gmail.com

Supplementary Information S1 – *Properties of MNPs used*

The transmission electron micrograph (TEM) and magnetization curve of MNPs employed in this study is tabulated in Figure S1. According to Figure S1, the diameter of MNPs is ~40 nm and the MNPs have saturation magnetization of 74.61 emu/g (or equivalent to 74.61 A.m^2/kg).

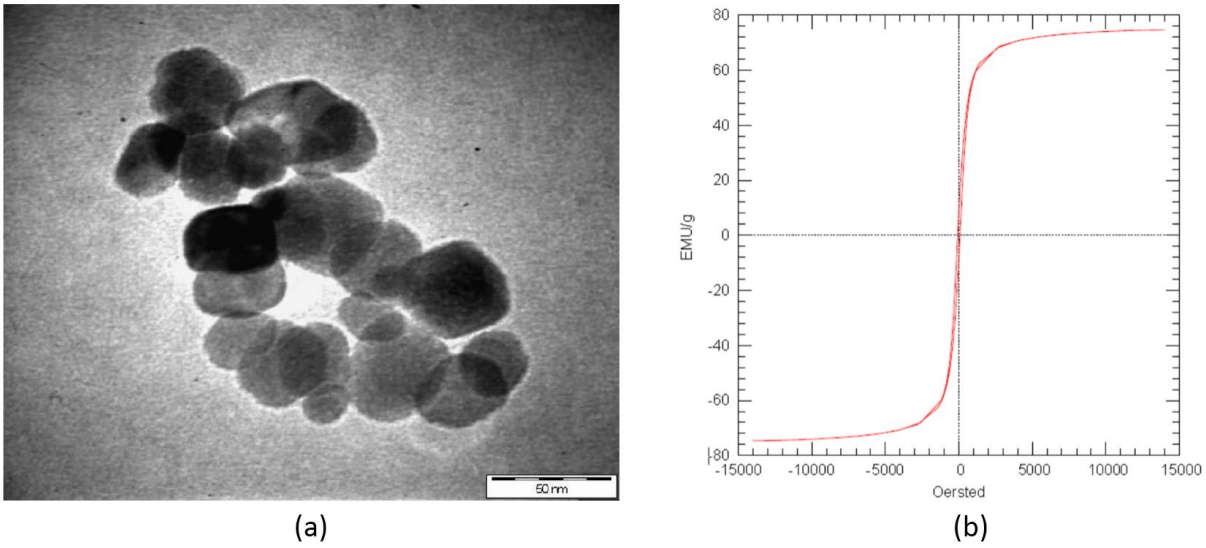

Figure S1: (a) Transmission electron micrograph (TEM) and (b) magnetization curve of iron oxide MNPs used in this study (reproduced with permission from ref. [1]**)**

Supplementary Information S2 – *Justification of Methylene Blue (MB) as an Effective Fluid Tracker in the Magnetophoresis Experiments in this Study*

Despite possessing the opposite electrostatic charge to PSS-functionalized MNPs, methylene blue molecule (MB) proves effective as a convective tracer in the magnetophoresis experiments conducted in this study, as supported by the following experiments.

Experiment (i): Concentration of MB Before and After Magnetophoresis of MNP Solution

We assessed the concentration of methylene blue (MB) in the MNP solution after subjecting it to magnetophoresis, comparing it with the concentration of a blank solution injected with the same amount of MB (without MNPs and occurrence of magnetophoresis). This analysis identifies the amount of MB remaining in the solution after magnetophoresis, representing the portion not absorbed by MNPs and separated from the solution. To achieve this, we measured the light absorbance of the MNP solution (initially injected with dye) at the end of the magnetophoresis process (when all MNPs have been successfully separated) using a UV-vis spectrophotometer (referred to as Sample 1). Subsequently, we injected the same amount of MB into a blank solution and measured the light absorbance of the uniformly dispersed MB in the solution (referred to as Sample 2). The results of this measurement are presented in the table below:

	Light Absorbance			
	Trial 1	**Trial 2**	**Trial 3**	**Average**
Sample 1	0.131	0.135	0.124	0.130
Sample 2	0.144	0.142	0.149	0.145

* The light absorbance of blank solution (without MB) has been set to be zero as a reference.

The average light absorbance of Sample 1 was found to be 0.130, while Sample 2 exhibited a light absorbance of 0.145. The diminished light absorbance in the solution after magnetophoresis is attributed to the lower concentration of MB, as some of the MB may have been electrostatically attracted to the MNPs and separated from the solution alongside the MNPs during magnetophoresis. Notably, the light absorbance for Sample 1 is only ~10% lower than that of Sample 2 (it's essential to note that the light absorbance of 0 is set for the blank solution, and the Beer-Lambert law is applicable within this concentration range). Therefore, by interpretating using Beer-Lambert law, approximately 10% of the MB was loss through the process, while the remaining 90% remains freely suspended in the solution, effectively serving as the convection tracker. Consequently, it can be inferred that MB effectively functions as a convective tracker during the magnetophoresis of the MNP solution in this study.

Experiment (ii): Hydrodynamic Diameter of MNP Clusters in Solution under the Presence and Absence of Methylene Blue (MB)

In addition, we have also tried to do the DLS analysis to measure the hydrodynamic diameter of the MNP clusters and the results are tabulated in the following table:

Sample	**Hydrodynamic Diameter (nm)**
PSS-functionalized MNP*	272
PSS-functionalized MNP (in MB dye solution)	276

** The hydrodynamic size of PSS-functionalized MNP produced by each experiment maybe varied within the range of 200-300 nm, thus, the hydrodynamic diameter here is different from the one reported in the main manuscript (we used different batch of functionalized MNP to perform this analysis).*

As evidenced by the results, the PSS-functionalized MNP, when MB is present, exhibits a slightly larger hydrodynamic size compared to the condition without injected MB. This marginal 1.5% increment in hydrodynamic size is likely attributable to a minor bridging effect. However, it's crucial to note that such a modest increment in the hydrodynamic diameter of MNP clusters is unlikely to exert a significant impact on the magnetophoresis kinetics.

Importantly, the injected MB effectively traces the fluid motion of the MNP solution during magnetophoresis despite this minor alteration.

Diffusion of MB in Relative to Induced Convection

In this subsection, we aim to make a basic assessment of the comparative scale of molecular diffusion for MB molecules in contrast to the magnetophoresis-induced convection. This evaluation is crucial to ascertain that the molecular diffusion of MB molecules does not dominate and impede their role as a convective tracer.

In this assessment, MB molecule is approximated as a rectangular volume with dimension of 17.0 × 7.6 × 3.3 Å [2]. Let us estimate the magnitude of the diffusive displacement of the MB molecules during the experiment for experiment set 1 (one of the experimental sets with the longest duration). Here, we assume that 3.3 Å (or 3.3×10^{-10} m) is the characteristic length of the MB molecules so that this estimation will give the highest possible diffusivity of MB molecules under the magnetophoresis experiment. Here, we also assume that the water has a viscosity of ~0.00089 Pa.s under room temperature (T = 300 K). According to Einstein-Stokes Equation, the diffusion coefficient of the particle can be estimated as:

$$D = \frac{kT}{6\pi\eta r} = \frac{1.38 \times 10^{-23}(300)}{6\pi(0.00089)(3.3 \times 10^{-10})} = 7.478 \times 10^{-10} m^2/s$$

Using this diffusion coefficient, we can estimate the magnitude of the diffusive displacement of the MB molecules under a stagnant fluid. Noting that the magnetophoresis experiment has a duration of about ~7200 seconds, the estimated diffusive displacement of MB molecule for experiment set 1 is:

$$d \approx \sqrt{2Dt} = \sqrt{2 \times 7.478 \times 10^{-10} \times 7200} \approx 3.28 \times 10^{-3} m$$

at the end of the experiment. In other word, the estimated diffusive velocity of the MB molecule is:

$$\frac{3.28 \times 10^{-3} m}{7200\ s} = 4.56 \times 10^{-7} m/s$$

which is much slower as compared to the magnetophoresis induced convection with the magnitude of 10^{-4} – 10^{-2} m/s (resulted from both experiment and simulation). Therefore, the dye motion the dye tracing experiment of our study is predominantly driven by the magnetophoresis induced convection rather than the molecular diffusion.

Supplementary Information S3 – *Justification of Poly(diallyldimethylammonium chloride) (PDDA) as an Effective Fluid Thickener in the Magnetophoresis Experiments in this Study*

To examine the efficacy of PDDA as a thickening agent in the PSS-functionalized MNP solution in our study, we conducted dynamic light scattering (DLS) measurements on the hydrodynamic size of MNP clusters in PDDA solutions, utilizing the highest concentration of 150 g/L of PDDA employed in our experiments. The results are summarized in the table below:

Sample	**Hydrodynamic Diameter (nm)**
PSS-functionalized MNP	272
PSS-functionalized MNP (in PDDA solution)	207
PSS-functionalized MNP (in PDDA + MB solution)	215

The results indicate a generally smaller hydrodynamic diameter of MNP clusters in the solution injected with the PDDA solution. This occurrence may be attributed to the excess amount of PDDA relative to the MNP in our system. For instance, even in the experimental set with the least amount of PDDA (experimental set 2 with 10 g/L of PDDA), the concentration of PDDA is substantially higher (approximately 167 times higher) than that of the MNP. It should be noted that the amount of PDDA would be much higher in the experiment sets 3 – 5, which involves the injection of more PDDA to create environment with the higher viscosity. Due to the excessive amount of cationic PDDA molecules, they adsorb onto the anionic PSS-functionalized MNP clusters, forming a PDDA layer on the clusters' surface, rendering it positively charged. Although there is still an excess of cationic PDDA molecules in the surrounding fluid, the electrostatic repulsion between the positively charged fluid (due to the excess cationic PDDA molecules) and the positively charged surface of the MNP cluster, due

to the PDDA layer, can lead to the contraction of the MNP clusters, resulting in a smaller hydrodynamic diameter as observed in the DLS measurements.

Hence, owing to the significantly excessive amount of PDDA present in the MNP solution, the PDDA molecules do not act as bridging molecules between neighboring MNP clusters; instead, they serve as a thickening agent in our study.

Supplementary Information S4 - *Viscosity Calibration*

The viscosity of the MNP solution is manipulated by dissolving different amounts of poly(diallyldimethylammonium chloride) (PDDA) into the solution. Thus, a calibration experiment was conducted to correlate the solution viscosity to the concentration of PDDA. The Brookfield DV2T viscometer was used to measure the viscosities of PDDA solution with different PDDA concentration. Pure PDDA (molecular weight of 400,000 - 500,000) purchased from Sigma-Aldrich Co. was mixed with deionized (DI) water to prepare solutions with different PDDA concentration: 0 g/L (pure water), 70 g/L, 80 g/L, 90 g/L, 100 g/L, 110 g/L, 120 g/L, 130 g/L, 140 g/L, 150 g/L and 200 g/L (pure PDDA). The viscosity measurement was taken at three different rotation speeds of the spindle (100 rpm, 150 rpm and 200 rpm) which corresponds to different shear rates (Figure S2(a)).

The viscosity of the quiescent PDDA solution was obtained by extrapolating the viscosity versus shear rate graph (Figure S2(a)) to the point where shear rate equal to zero. The relationship between the viscosity of quiescent PDDA solution and PDDA concentration is tabulated in Figure S2(b). A rise in the viscosity was observed when concentration of the PDDA increases. The increase in viscosity (thickening) with PDDA concentration is caused by the strong internal friction of the randomly coiled and entangled PDDA polymer molecules which have high molecular weight (M_w ~ 400,000 – 500,000). The long PDDA molecules becomes crowded as the PDDA concentration increases which gives rise to more significant overlap and entanglements of segments of polymer chains, which in turn imposing higher resistance to the fluid flow. The relationship between viscosity and concentration of PDDA solution is fitted into a quadratic function (see Figure S2(b)), in which coefficient of determination R^2 value is equal to 0.9941. Thus, this empirical correlation is reliable to predict the viscosity of MNP solutions that were added with specific amount of PDDA in the magnetophoresis experiment.

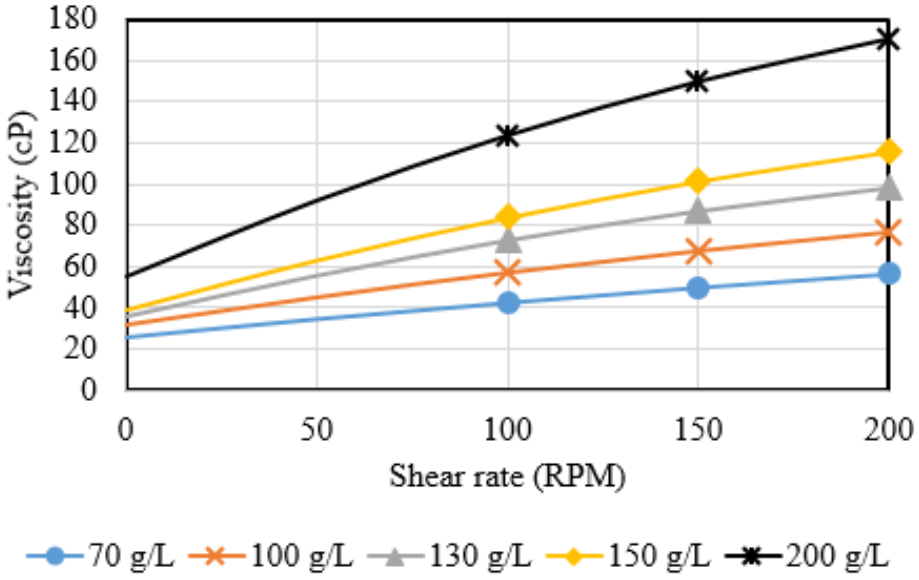

(a)

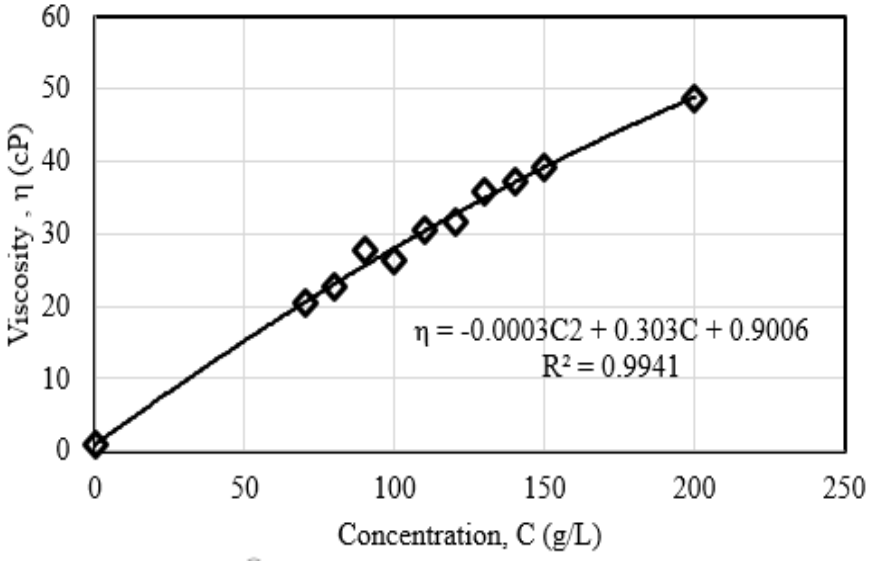

(b)

Figure S2: (a) Measured viscosity of solution with different PDDA concentration at different shear rates. The graphs were extrapolated backwards to obtain viscosity values at zero shear rate (quiescent fluid). The data were then plotted in (b), which shows the relationship between the viscosity of the solution (under quiescent condition) and the PDDA concentration.

Supplementary Information S5 – ***Mathematical Modelling of Magnetophoresis under the Presence of Magnetophoresis Induced Convection***

The mass transfer of MNP within the MNP solution is governed by diffusion-convection equations as indicated below [3]:

$$\frac{\partial c}{\partial t} = D\nabla^2 c - \nabla \cdot (\vec{v}c) \qquad (S1)$$

where D is the diffusion coefficient of MNP, c is the MNP concentration and $\vec{v}$ is the convective velocity field. On the right-hand side of Equation (S1), the first and second terms correspond to the mass transport of MNPs due to diffusion and convection modes, respectively [4]. Here, the convective velocity $\vec{v}$ is the velocity of MNP solution (the combination of fluid and MNPs) which is viewed as a continuum. In other words, it has been assumed that the magnetophoresis induced convection is dominant in all magnetophoresis processes conducted in this study (which is the case as shown in the results demonstrated in Section 4 of the main text). Also, in this model, hydrodynamic interaction between MNPs and surrounding fluid (momentum transfer among them) during magnetophoresis has been accounted by the incorporation of fluid flow equations (incompressible continuity equation and modified Navier-Stokes equation) as shown below [5]:

$$\nabla \cdot \vec{v} = 0 \qquad (S2)$$

$$\rho\left[\frac{\partial \vec{v}}{\partial t} + \vec{v}(\nabla \cdot \vec{v})\right] = -\nabla p + \eta\nabla^2\vec{v} + \rho\vec{g} + \overrightarrow{f_m} \qquad (S3)$$

where ρ is the density of MNP solution, p is the absolute pressure, η is the dynamic viscosity, $\vec{g}$ is the acceleration due to gravity and $\overrightarrow{f_m}$ is the volumetric magnetic force acting on MNP solution under the presence of an external magnetic field. Here, the magnetic force term $\overrightarrow{f_m}$ can be related to the particle concentration c and magnetic field gradient ∇B as given by [4]:

$$\overrightarrow{f_m} = M\nabla B = cM_{p,m}\nabla B \qquad (S4)$$

where M is the volumetric magnetization of the MNP solution and $M_{p,m}$ is the magnetization per unit mass of MNP. Owing to the superparamagnetic nature of the MNPs adopted in this study (see Figure S1(b) in Supplementary Information S1), the magnetization of MNP can be described by a Langevin function as shown below [6]:

$$M_{p,m} = M_s L\left(\frac{mB}{\mu_0 k_B T}\right) = M_s\left[coth\left(\frac{mB}{\mu_0 k_B T}\right) - \frac{\mu_0 k_B T}{mB}\right] \qquad (S5)$$

where M_s is the saturation magnetization (per unit mass) of MNP, B is the magnetic field strength, μ_0 is the permeability of free space, k_B is the Boltzmann's constant and T is the absolute temperature. There is an unknown m in this equation which can be evaluated by fitting magnetization curve in Figure S1(b) with the Langevin function (see Supplementary Information S6 for more detailed elaboration). On the other hand, the magnitude of magnetic field strength generated by cylindrical magnet can be computed by using the following equation [7]:

$$B = B(y) = \frac{B_r}{2}\left[\frac{y+h}{\sqrt{(y+h)^2 + r^2}} - \frac{y}{\sqrt{y^2 + r^2}}\right] \qquad (S6)$$

where B_r is the remanent magnetization of magnet, h is the height of magnet, r is the radius of magnet and y is the distance from the magnet pole. In this simulation, the magnetic field strength is assumed to be varied along the vertical direction (y-direction) and constant along the horizontal direction (x-direction). Owing to this assumption, we could further simplify the orientation of the magnetic field gradient by taking it as purely pointing towards the y-direction throughout the entire MNP solution, as given by the following equation [4]:

$$\nabla B \approx \frac{\partial B}{\partial y}\overrightarrow{\boldsymbol{e_y}} = \frac{B_r r^2}{2}\left[\frac{1}{[(y+h)^2 + r^2]^{\frac{3}{2}}} - \frac{1}{[y^2 + r^2]^{\frac{3}{2}}}\right]\overrightarrow{\boldsymbol{e_y}} \qquad (S7)$$

where $\overrightarrow{\boldsymbol{e_y}}$ is the unit vector pointing to the positive *y*-direction.

Regarding to the boundaries, no-slip condition is applied to all the four boundaries of MNP solution such that the fluid velocity is always zero ($\vec{\boldsymbol{v}} = 0$) at these boundaries (Figure 2 in the main text) [8]. Additionally, the top, left and right sides of the boundary are assumed to be impenetrable, i.e. there is no MNP flowing across these three boundaries (labelled as red colour in Figure 2 in the main text). However, there is an outlet flux of the MNPs at the bottom boundary, which corresponds to the continuous withdrawal of MNPs from their suspension at the collection plane, as formulated by the following equation [4,9]:

$$J = \frac{c_0 V_s k}{A_s} e^{-kt} \qquad (S8)$$

where c_0 is the initial MNP concentration, V_s is the volume of MNP solution, A_s the is surface area of the MNP collection plane (which is the bottom surface of the cuvette at $y = 0$) and k is the rate constant given by [9]:

$$k = \frac{v_y\big|_{y=0} A_s}{V_s} \qquad (S9)$$

Here, $v_y\big|_{y=0}$ is the magnetophoretic velocity of MNP aggregates at the MNP collection plane. It should be noted that Equation (S9) is formulated by assuming that the MNP solution remains homogeneous in term of particle concentration throughout the entire magnetophoresis process, which can serve as a good approximation for the current study to investigate the relationship between some critical design parameters and intensity of magnetophoresis induced convection.

Up to this point, it should be emphasized that the MNP clusters will undergo further aggregation (either reversible or irreversible) upon subjected to external magnetic field during the magnetophoresis process, thus, MNP aggregates are formed (see Supplementary Information S7 and S8 for the detail calculation to prove the existence of particle aggregation

in our MNP system). Thus, in this paper, MNP aggregate is the term used to denote a collection of a number of MNP clusters resulted from the magnetically-induced aggregation (we assumed elongated MNP chains are formed as reported by ref. [10]). The magnetophoretic velocity of MNP aggregate $v_y\big|_{y=0}$ can be calculated by using the force balance principle on a MNP aggregate at the collection plane:

$$F_{mag}\big|_{y=0} = F_d|_{y=0} \tag{S10}$$

where $F_{mag}\big|_{y=0}$ and $F_d|_{y=0}$ are the magnetic and viscous drag forces imposed on a MNP aggregate at the MNP collection plane. As both aforementioned forces can be expressed as:

$$F_{mag}\big|_{y=0} = m_{ag}\nabla B|_{y=0} \tag{S11}$$

$$F_d|_{y=0} = \zeta^{'}\,\eta\, v_y\big|_{y=0} \tag{S12}$$

Equation (S10) can be rewritten and rearranged as follows:

$$m_{ag}\nabla B|_{y=0} = \zeta^{'}\,\eta\, v_y\big|_{y=0} \tag{S13a}$$

$$v_y\big|_{y=0} = \frac{m_{ag}\nabla B|_{y=0}}{\zeta^{'}\eta} \tag{S13b}$$

Here, $\zeta^{'}$ is the friction coefficient of MNP aggregate (which is geometrical dependent) and m_{ag} is the magnetic dipole moment possessed by one MNP aggregate. Upon substitution of Equation (S13b) into Equation (S9), the following equations are obtained:

$$k = \frac{m_{ag}\nabla B|_{y=0} A_s}{\zeta^{'}\eta V_s} \tag{S14a}$$

$$\frac{m_{ag}}{\zeta^{'}} = \frac{\eta V_s k}{\nabla B|_{y=0} A_s} \tag{S14b}$$

Since the magnitude of m_{ag} and $\zeta^{'}$ is only dependent on the physical properties of MNPs (such as saturation magnetization, size and geometrical shape of MNP aggregates) at the collection plane, the $\frac{m_{ag}}{\zeta^{'}}$ term on the left hand side of Equation (S14b) is assumed to have the same magnitude for all experimental sets being conducted in this study (we employed the same particle for all experimental sets). This is a reasonable assumption because all MNPs achieve saturation magnetization and the number of MNP clusters per aggregates has been reaching a steady state under the relatively high magnetic field at the MNP collection plane (see Supplementary Information S7 and S9 for the calculation details). Therefore, we employed the rate constant *k* deduced from the results of one of our experimental sets (Set 8 in Table 1) to estimate the value of $\frac{m_{ag}}{\zeta^{'}}$, which is then being used to calculate the rate constant for the simulation of the other experimental sets by Equation (15a). The detailed calculation is demonstrated in Supplementary Information S9. In addition, it is also found out that the number of MNP clusters in one MNP aggregate is given by 32 for the MNP system that is employed in this study (see Supplementary S10 for the calculation details).

As the initial condition is concerned, the fluid is assumed to be stagnant ($\vec{v}$ = 0) and MNP concentration is uniform throughout the solution at value of $c_{0,mol}$ before the initiation of magnetophoresis. In addition, the pressure at the MNP solution surface ($y = H$ cm, where H is the height of MNP solution filled in the cuvette) is set at atmospheric pressure P_0, in which the pressure in the MNP solution is calculated by:

$$P = P_0 + d_{solution}\rho g \qquad (S15)$$

where $d_{solution}$ is the depth of the MNP solution. The model was computed numerically with COMSOL Multiphysics.

Supplementary Information S6 - *Fitting Magnetization Curve*

The strength of magnetic moment for one magnetic dipole (the *m* value in Langevin function, as indicated by Equation (S5)) was obtained by employing the magnetization curve as shown in Figure S1(b). The raw data from magnetization curve (Figure S1(b)) was fitted into the Langevin function, which is tabulated in Figure S3. The error of the fitting values is ranging from 0.2 to 4.8%, with the *m* value of 1.9×10^{-25} J·m/A.

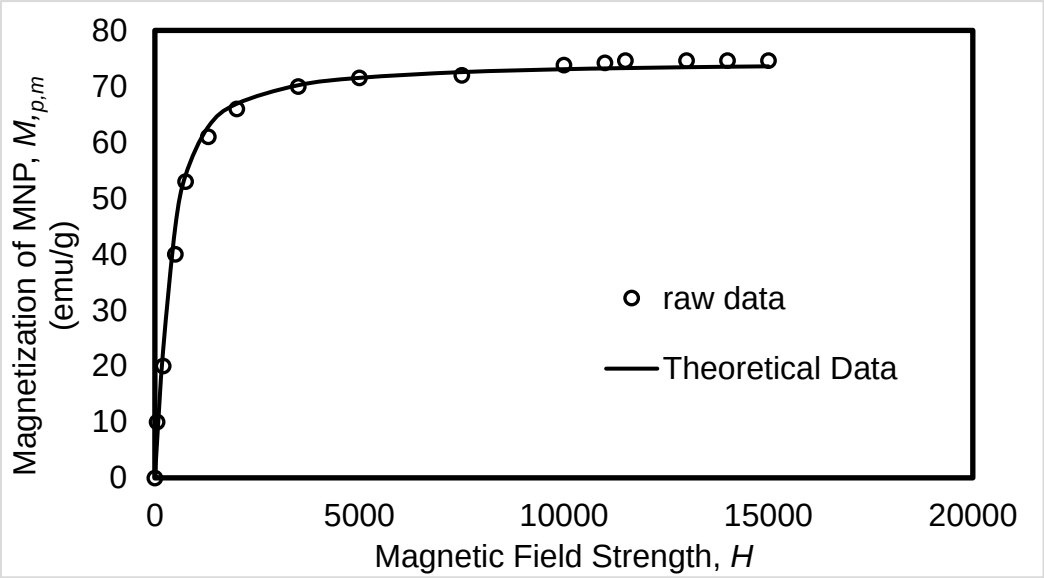

Figure S3. The fitting of magnetization data (of MNP used in the current study) by using the Langevin function.

Supplementary Information S7 – *Calculation for Properties of PSS-functionalized MNP (MNP Clusters)*

In article, the following terminologies are used to denote MNPs of different aggregation states in our model system:

- **Bare MNP** – the single MNP without undergoing functionalization or aggregation. The diameter of the MNP is about 40 nm (see Figure S1(a)).
- **MNP cluster** – the cluster of MNP resulted after functionalizing with PSS. It consists of multiple bare MNPs that are interlinked among each other by PSS molecules. The MNP cluster has hydrodynamic size of 234.9 nm according to the DLS measurement (see Figure 3 of the main text).
- **MNP aggregate** – it is resulted from the aggregation of MNP clusters induced by the magnetization effect of MNP during magnetophoresis – which is also known as cooperative effect of magnetophoresis.

The calculation of the property of PSS-functionalized MNP (or MNP cluster) begins with the magnetization curve of the MNP system obtained from ref. [11] (the MNPs in current study possess of same specification and purchased from the same supplier as MNPs reported in this work). The magnetization curves of bare (unfunctionalized) MNP and PSS-functionalized MNP are tabulated in Figure S4. According to Figure S4, the saturation magnetization value, M_s, of bare MNP and PSS-functionalized-MNP is given by ~75 and ~70 emu/g, respectively.

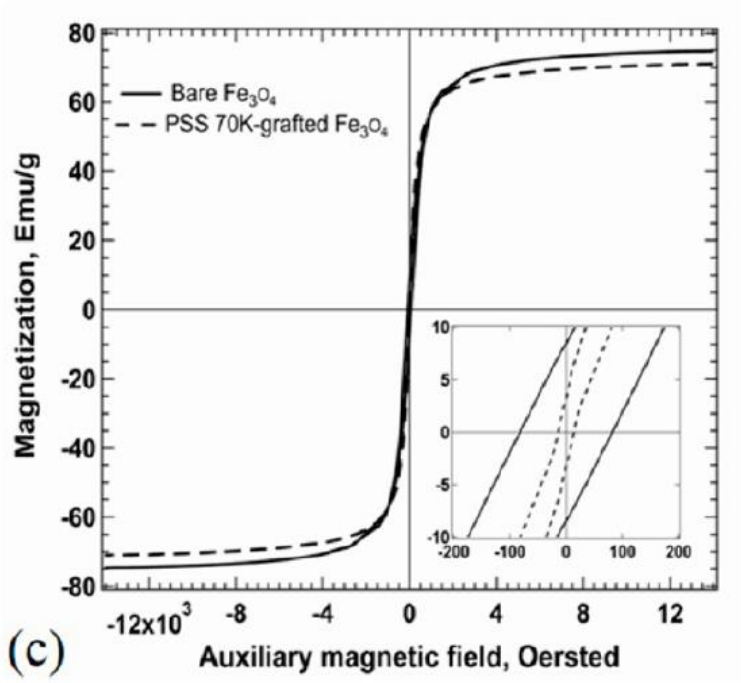

Figure S4: Magnetization curves of bare MNP and PSS-functionalized MNP from ref. [11] **which have the same specification with the MNP system used in this study.**

By assuming the magnetic response is entirely originated from the MNP (PSS does not contribute any magnetic response), the mass fraction of MNP within the PSS-functionalized MNP can be estimated as follows:

Mass Fraction of MNP in PSS-functionalized MNP cluster = $\frac{70\ emu/kg}{75\ emu/kg} \times 100\%$

= 93.33 wt%

Mass Fraction of PSS in PSS-functionalized MNP cluster = 100 – 93.33

= 6.67 wt%

By taking the packing factor of the MNP clusters is 0.74 (the highest packing factor of uniform-sized spherical objects, which indicates 74 vol% of the MNP cluster is occupied by MNP or PSS), density of MNP is 5180 kg/m^3 and density of PSS is 810 kg/m^3, the volume fraction of MNPs in the cluster can be estimated as follows:

Volume Fraction of MNP in PSS-functionalized MNP cluster = $\frac{\frac{0.933}{5180\ kg/m^3}}{\frac{0.933}{5180\ kg/m^3}+\frac{0.0667}{810\ kg/m^3}} \times 0.74$

$= 0.5064$

Next, the mass of magnetic material (or MNP) can be estimated:

Volume of MNP in one PSS-functionalized MNP cluster , $V_{cluster}$

$$= \frac{\pi {d_{cluster}}^3}{6} \times\ 50.64\%$$

$$= \frac{\pi(234.9 \times 10^{-9})^3}{6} \times 0.5064$$

$$= 3.437 \times 10^{-21} m^3$$

Mass of MNP in one PSS-functionalized MNP cluster, $m_{cluster}$

$$= V_{cluster}\rho = 3.437 \times 10^{-21} \times 5180$$

$$= 1.78 \times 10^{-17} kg$$

Supplementary Information S8 – ***Estimation of Aggregation Parameter N* for MNP System used in Current Study***

Aggregation parameter, *N** is a dimensionless parameter that describes the degree of interaction among particles (with net magnetization) in fluid, which is formulated as follows [12,13]:

$$N^* = \sqrt{\emptyset_0 e^{\Gamma-1}} \qquad (S16)$$

where $\emptyset o$, is the volume fraction of particles in the solution and Γ is magnetic coupling parameter. Here, magnetic coupling parameter is defined as the ratio of magnetic energy to thermal energy when the two particles are at the close contact:

$$\Gamma = \frac{\mu_0 m_{MNP}^2}{2\pi d^3 k_B T} \qquad (S17)$$

where m_{MNP}^2 is magnetic dipole moment of particle. By assuming the MNP system in our study consists of the suspension of MNP clusters (which are PSS-functionalized-MNPs) in solution that have achieved saturation magnetization ($M_{p,m,sat}$ ~74.61 A.m^2/kg) with concentration of 40 mg/L (the lowest concentration of MNP as in our experiment), aggregation parameter is calculated as follows:

$$m_{cluster,sat} = m_{cluster} M_{p,m,sat}$$

$$= (1.78 \times 10^{-17} kg)(74.61 \text{ A.m}^2/\text{kg})$$

$$= 1.328 \times 10^{-15} \text{ A.m}^2$$

$$\Gamma = \frac{\mu_0 m_{cluster,sat}^2}{2\pi d_{cluster}^3 k_B T} \qquad [We\ assume\ m_{MNP}\ in\ Equation\ (S17) = m_{cluster,sat}]$$

$$= \frac{1.257 \times 10^{-6} \times (1.328 \times 10^{-15})^2}{2\pi \times (234.9 \times 10^{-9})^3 \times 1.38 \times 10^{-23} \times 300}$$

$$= 6573$$

$$\emptyset_0 = \frac{c}{\rho_p}$$

$$= \frac{0.04}{5180 \times 0.5064}$$

$$= 1.525 \times 10^{-5}$$

$$N^* = \sqrt{\emptyset_0 e^{\Gamma - 1}}$$

$$= \sqrt{(1.525 \times 10^{-5}) e^{6573-1}}$$

$$= 4.823 \times 10^{1424} \gg 1$$

The *N** value calculated is extreme huge (even larger than the number of atoms in the universe), thus, it can be deduced that the cooperative effect is very significant even in the magnetophoresis experiments by using the MNP solution with lowest concentration in this study. In other words, the MNP clusters can form a very large aggregate (which consists of 4.823×10^{1424} MNP clusters) if it is given sufficient time and MNP clusters to achieve aggregation equilibrium. However, the timescale needed to achieve the aggregation equilibrium state can be very much larger than our magnetophoresis duration, hence, we are not observing the attainment of aggregation equilibrium in our magnetophoresis experiments. Furthermore, the amount of MNP clusters in our MNP system is far lesser than the calculated *N** value, which subsequently renders MNP system has insufficient MNP clusters to achieve

the theoretical aggregation equilibrium state. However, the purpose of the calculation is to determine the nature of MNP interaction in our MNP system, and $N^* > 1$ indicates the cooperative effect of MNPs is substantial in the magnetophoresis experiments conducted in this study.

Supplementary Information S9 – *Calculation Details for Model Simulation*

A. Initial Molar Concentration, $c_{o,mol}$

As the 'Transport of Diluted Species' physics in COMSOL Multiphysics is using mole basis to calculate the transport behavior of a species to be studied, it is necessary to convert the concentration of MNP from mass to mole basis. First, the volume and mass of bare MNP ware calculated as follows:

$$Volume\ of\ bare\ MNP, V_{particle} = \frac{\pi d_{particle}^3}{6} = \frac{\pi(40 \times 10^{-9})^3}{6} = 3.351 \times 10^{-23} m^3$$

$$Mass\ of\ bare\ MNP, m_{particle} = V_{particle}\rho = 3.351 \times 10^{-23} \times 5180 = 1.736 \times 10^{-19} kg$$

If the initial mass concentration of MNP is given by $c_{0,mg/L}$ mg/L (or $c_{o,mass} = c_{0,mg/L}/1000$ kg/m^3), then the initial molar concentration is:

$$c_{o,mol} = \frac{c_{o,mass}}{m \times N_A} = \frac{c_{o,mg/L}/1000}{1.736 \times 10^{-19} \times 6.02 \times 10^{23}} = 9.5687 \times 10^{-9} c_{0,mg/L}\ mol/m^3 \quad (S18)$$

According to Equation (S18), the initial molar concentration used in our simulation is given by Table S1.

Table S1: The values of $c_{o,mol}$ to be used in the simulation of all experimental sets in this study.

$c_{0,mg/L}$ (mg/L)	$c_{o,mol}$ (mol/m^3)	Experimental Sets (see Table 1 in the main article)
40	3.827×10^{-7}	1 - 5
60	5.741×10^{-7}	6 - 11

B. Coefficient of Diffusion, *D*

In our simulation, the coefficient of diffusion is calculated according to the MNP cluster (not MNP aggregate). This assumption is made due to the relatively fast decay in magnetic field strength ∇B with respect to the distance from the magnet. For instance, the magnitude of ∇B decay from 95.74 T/m to 17.50 T/m when we are moving from magnet pole (y = 0) by only 1 cm along the axis (to y = 1 cm), when Magnet S is adopted. In other words, the MNP clusters might move individually (no chaining happens) in most regions of the MNP solution, especially when the container with height of 7 cm is used. Thus, the coefficient of diffusion for this simulation (which is needed in Equation (S2) of the main article) is approximated from Stokes-Einstein Equation as follows:

$$D = \frac{k_B T}{3\pi\eta d_{cluster}} = \frac{1.38 \times 10^{-23}(300)}{3\pi\eta(234.9 \times 10^{-9})} = \frac{1.87 \times 10^{-15}}{\eta} m^2/s \qquad (S19)$$

By using Equation (S19), the coefficient of diffusion of MNPs under solution of different viscosity is computed and tabulated in Table S2.

Table S2: The values of viscosity η and coefficient of diffusion *D* to be used in the simulation of all experimental sets in this study.

η (Pa.s)	*D* (m^2/s)	Experimental Sets (see Table 1 in the main article)
0.89	2.101×10^{-12}	1, 6 - 11
3.9	4.795×10^{-13}	2
15.3	1.222×10^{-13}	3
28.2	6.631×10^{-14}	4
39.6	4.722×10^{-14}	5

C. MNP Outward Flux at MNP Collection Plane, *J*:

According to the time-lapsed images of experiment set 8 (Figure S5(b) in Supplementary Information S12), the separation time of the order of ~10 minutes was observed. Thus, we used this experiment to estimate the size of the MNP aggregates that are formed in all experimental sets. This is because the significance of aggregation is entirely dependent on the particle magnetization, which has been almost reaching saturation magnetization at the MNP collection plane regardless of the dimension of magnet used in this study. For instance, Magnets S and B impose magnetic field strength of 0.6570 T and 0.6485 T on the MNP collection plane, which causes the MNP to gain magnetization $M_{p,m}$ of 71.50 A m^2 and 71.45 A m^2, respectively. The calculation details are demonstrated below:

Magnet S

Height of magnet, h = 1.5 cm = 0.015 m

Diameter of magnet, d = 1.4 cm = 0.014 m (Radius of magnet, r = 0.7 cm = 0.007 m)

Thus, the magnetization of MNP at the MNP collection plane (y = 0) is computed as follows:

$$B|_{y=0} = \frac{B_r}{2}\left[\frac{y+h}{\sqrt{(y+h)^2+r^2}} - \frac{y}{\sqrt{y^2+r^2}}\right]$$

$$= \frac{1.45}{2}\left[\frac{0+0.015}{\sqrt{(0+0.015)^2+0.007^2}} - \frac{0}{\sqrt{0^2+0.007^2}}\right] = 0.6570\ T$$

$$H = \frac{B}{u_0} = \frac{0.6570}{1.2568\times10^{-6}} = 5.228\times10^5$$

$$M_{p,m} = M_s L\left(\frac{mH}{k_B T}\right) = M_s\left[coth\left(\frac{mH}{k_B T}\right) - \frac{k_B T}{mH}\right]$$

$$= 74.61\left[coth\left(\frac{1.9\times10^{-25}(5.228\times10^5)}{1.381\times10^{-23}(300)}\right) - \frac{1.381\times10^{-23}(300)}{1.9\times10^{-25}(5.228\times10^5)}\right]$$

$$= 71.50\ A\cdot m^2/kg$$

Magnet B

Height of magnet, h = 4.0 cm = 0.04 m

Diameter of magnet, d = 4.0 cm = 0.04 m (Radius of magnet, r = 2.0 cm = 0.02 m)

Thus, the magnetization of MNP at the MNP collection plane (y = 0) is computed as follows:

$$B|_{y=0} = \frac{B_r}{2}\left[\frac{y+h}{\sqrt{(y+h)^2+r^2}} - \frac{y}{\sqrt{y^2+r^2}}\right]$$

$$= \frac{1.45}{2}\left[\frac{0+0.04}{\sqrt{(0+0.04)^2+0.02^2}} - \frac{0}{\sqrt{0^2+0.02^2}}\right] = 0.6485\ T$$

$$H = \frac{B}{u_0} = \frac{0.6485}{1.2568\times10^{-6}} = 5.160\times10^5$$

$$M_{p,m} = M_s L\left(\frac{mH}{k_B T}\right) = M_s\left[coth\left(\frac{mH}{k_B T}\right) - \frac{k_B T}{mH}\right]$$

$$= 74.61\left[coth\left(\frac{1.9\times10^{-25}(5.160\times10^5)}{1.381\times10^{-23}(300)}\right) - \frac{1.381\times10^{-23}(300)}{1.9\times10^{-25}(5.160\times10^5)}\right]$$

$$= 71.46\ A\cdot m^2/kg$$

Here, we used Equation (S14b) from Section S3 and experimental observation from Set 8 to estimate the properties of MNP aggregates on MNP collection plane. Here, we fix the time constant ($\tau = 1/k$) as 10 minutes (or 600 s), which is the timescale of the separation process:

$$\mathrm{k} = \frac{1}{600}\ s^{-1}$$

Additionally, the other values of properties needed in Equation (15b) are shown below:

Viscosity:

η = 0.00089 Pa.s

Volume of MNP solution used:

V_s = 7 mL = 7 × 10^{-6} m^3

Area of MNP collection plane:

A_s = 1 cm × 1 cm = 1 × 10^{-4} m^2

Magnetic field gradient:

$$\nabla B|_{y=0} = \frac{B_r r^2}{2}\left[\frac{1}{[(y+h)^2+r^2]^{\frac{3}{2}}} - \frac{1}{[y^2+r^2]^{\frac{3}{2}}}\right] \qquad (For\ Magnet\ B)$$

$$= \frac{1.45 \times 0.02^2}{2}\left[\frac{1}{[(0+0.04)^2+0.02^2]^{\frac{3}{2}}} - \frac{1}{[0^2+0.02^2]^{\frac{3}{2}}}\right]$$

$$= 33.01\ T/m$$

By inserting the values above into Equation (S14b),

$$\frac{m_{ag}}{\zeta'} = \frac{(0.00089)(7\times10^{-6})(1/600)}{(33.01)(1\times10^{-4})} = 3.146\times10^{-9}\,\mathrm{A\cdot m\cdot s} \qquad (S20)$$

The magnitude of $\frac{m_{ag}}{\zeta'}$ is assumed to be the same in other experimental sets, thus, Equation (S14a) can be rewritten as follows to estimate the rate constant *k* for the simulation of the other experimental sets:

$$k = \frac{m_{ag}\nabla B|_{y=0} A_s}{\zeta'\eta V_s} = 3.146\times10^{-9}\frac{\nabla B|_{y=0} A_s}{\eta V_s} \qquad (S21)$$

By applying Equation (S8), the separation flux of MNPs (in mole basis) at the collection plane can be formulated as:

$$J = \frac{c_0 V_s k}{A_s}e^{-kt} = 3.146\times10^{-9}\frac{9.5687\times10^{-9} c_{0,mg/L}\nabla B|_{y=0}}{\eta}e^{-kt}$$

$$= 3.01\times10^{-17}\frac{c_{0,mg/L}\nabla B|_{y=0}}{\eta}e^{-kt}$$

$$= J_{0,mol}e^{-kt}$$

where:

$$J_{0,mol} = 3.01\times10^{-17}\frac{c_{0,mg/L}\nabla B|_{y=0}}{\eta} \qquad (S22)$$

which is the MNP flux at the collection plane (in mole basis). Table S3 tabulates the essential values used in the simulation:

Table S3: The values of viscosity η and coefficient of diffusion D to be used in the simulation of all experimental sets in this study.

Experimental Set	$\nabla B\|_{y=0}$ (T/m)	D (m^2/s)	k (s^{-1})	$J_{0,mol}$ (mol/m^2.s)
1	95.74	2.10×10^{-12}	8.46×10^{-3}	1.94×10^{-10}
2	95.74	4.79×10^{-13}	1.93×10^{-3}	4.43×10^{-11}
3	95.74	1.22×10^{-13}	4.92×10^{-4}	1.13×10^{-11}
4	95.74	6.63×10^{-14}	2.67×10^{-4}	6.13×10^{-12}
5	95.74	4.72×10^{-14}	1.90×10^{-4}	4.37×10^{-12}
6	33.01	2.10×10^{-12}	1.67×10^{-3}	4.47×10^{-11}
7	33.01	2.10×10^{-12}	1.67×10^{-3}	4.47×10^{-11}
8	33.01	2.10×10^{-12}	1.67×10^{-3}	4.47×10^{-11}
9	33.01	2.10×10^{-12}	1.67×10^{-3}	4.47×10^{-11}
10	95.74	2.10×10^{-12}	4.83×10^{-3}	1.29×10^{-10}
11	95.74	2.10×10^{-12}	4.83×10^{-3}	1.29×10^{-10}

D. Volumetric Magnetic Force, $\overrightarrow{f_m}$

The volumetric magnetic force $\overrightarrow{f_m}$ is computed from Equation (S4), which can be related to the molar concentration of MNP (the concentration used in our simulation) as follows:

$$\begin{aligned}\overrightarrow{f_m} = cM_{p,m}\nabla B &= c_{mol}N_A m_{particle}M_{p,m}\nabla B \\ &= c_{mol}(6.02 \times 10^{23})(1.736 \times 10^{-19})M_{p,m}\nabla B \\ &= 1.045 \times 10^5 c_{mol}M_{p,m}\nabla B \end{aligned} \quad (S23)$$

Supplementary Information S10 – *Calculation of MNP Aggregates Size*

Though the size of the effective MNP aggregate is not necessary for the simulations, an estimation is in order. Under saturation magnetization, the saturation magnetization of MNPs $M_{p,m}$ is ~71.50 Am^2/kg (see Supplementary Information S9, Section C), thus, the magnetic moment contained in one MNP cluster at MNP collection plane $m_{cluster|y=0}$ is given by:

$$m_{cluster|y=0} = m_{cluster}M_{p,m} = (1.78 \times 10^{-17}\ kg)(\ 71.50\ Am^2/kg) = 1.273 \times 10^{-15}\ Am^2$$

where $m_{cluster}$ is mass of one MNP cluster (the calculation details are shown in Supplementary Information S7). Let us assume a slender aggregate is formed with N MNP clusters (cluster diameter $d_{cluster}$ =234.9 nm), so that the MNP aggregate is possessing magnetic moment $m_{ag} = Nm_{cluster|y=0}$. Slender body theory yields for the longitudinal friction coefficient ζ' of a chain with length L and diameter $d_{cluster}$ as formulated by:

$$\zeta' = \frac{2\pi L}{\ln\left(\frac{2L}{d_{cluster}}\right) - \frac{1}{2}} \qquad (S24)$$

For a single MNP aggregate chain, $L = Nd_{cluster}$, thus, we have:

$$\frac{m_{ag}}{\zeta'} = \frac{Nm_{cluster|y=0}}{2\pi N d_{cluster}}\left[(\ln(2N) - \frac{1}{2}\right] \qquad (S25)$$

By using the values of $\frac{m_{ag}}{\zeta'}$, $m_{cluster|y=0}$ and $d_{cluster}$ in Equation (S25), it can be found that $N \approx 32$. Therefore, it can be estimated that there are about 30 MNP clusters residing in one MNP aggregate induced by the external magnetic field at MNP collection plane.

Supplementary Information S11 – *Estimation of Magnetophoretic Velocity of MNP Aggregates*

Following the calculation from the previous section, we can proceed furthermore to calculate the magnetophoretic velocity of individual MNP aggregates upon the exposure to the magnetic field. As magnetic dipole moment of one MNP cluster (PSS-functionalized MNP) at saturation is 1.273×10^{-15} A m^2 and average number of MNP clusters per MNP aggregate N is 32, we can calculate the length of MNP aggregates (which is assumed to be in the elongated form), L, is given by:

$$L = Nd_{cluster} = 32 \times 234.9 \times 10^{-9} = 7.516 \times 10^{-6} \text{ m}$$

Then, we can calculate the longitudinal friction coefficient of the elongated aggregate ζ' (by using Equation (S24)):

$$\zeta' = \frac{2\pi L}{\ln\left(\frac{2L}{d_{cluster}}\right) - \frac{1}{2}} = \frac{2\pi(7.516 \times 10^{-6})}{\ln\left(\frac{2(7.516 \times 10^{-6})}{234 \times 10^{-9}}\right) - \frac{1}{2}} = 1.2906 \times 10^{-5}$$

The magnetic dipole moment of one MNP aggregate also can be calculated as follows:

$$m_{agg} = 32 \times 1.273 \times 10^{-15} = 4.0736 \times 10^{-14} \text{ Am}^2$$

To calculate the magnetophoretic velocity of individual MNP aggregate during magnetophoresis, we employ the balance of magnetic and viscous forces acting on the MNP aggregate, with magnetic field gradient ∇B = 95.74 T/m (the highest magnetic field gradient employed in the current study, which is at the collection plane under magnet S, see Figure 11 in the main manuscript) and viscosity η = 0.00089 Pa.s:

$$F_{mag} = F_{drag}$$

$$m_{agg}\nabla B = \zeta' \eta v_{agg}$$

$$(4.0736 \times 10^{-14})(95.74) = (1.2906 \times 10^{-5})(0.00089)v_{agg}$$

$$v_{agg} = 3.4 \times 10^{-4} \text{ m/s}$$

In addition, at the point which is located 1 cm away from the magnet pole (y = 1 cm), ∇B has been decayed to 17.5 T/m, and the magnetophoretic is estimated as 6.2×10^{-5} m/s by using the above calculation method.

Supplementary Information S12 – *Estimation of Temperature Rise due to Viscous Dissipation on Magnetophoresis of MNP Solution*

This section is intended to estimate the temperature rise in MNP solution resulted from the viscous dissipation. In this calculation. it is assumed that the entire solution is slowed down and finally stopped (final velocity = 0) after the dissipation process, so that the temperature rise produced from the maximum dissipation can be estimated. After the dissipation process, the kinetic energy of the convection flow is converted to the thermal energy of MNP solution. The change in kinetic energy is given by:

$$\Delta KE = \frac{1}{2}M(v_f^2 - v_i^2)$$

where M is the mass of MNP solution, v_f is the final velocity and v_i is the initial velocity. On the other hand, the change in thermal energy is given by:

$$\Delta TE = MC_p\Delta T$$

where C_p is the specific heat capacity of MNP solution and ΔT is the temperature change of MNP solution. According to the conversation of energy:

$$\Delta KE + \Delta TE = 0$$

$$\frac{1}{2}M\left(v_f^2 - v_i^2\right) + MC_p\Delta T = 0$$

$$\frac{1}{2}\left(v_f^2 - v_i^2\right) + C_p\Delta T = 0 \qquad (S26)$$

Here, we let v_f = 0 (full dissipation is assumed), v_i = 10^{-2} m/s (typical magnitude of induced convection) and C_p = 4200 J/(kg·°C). By substituting these values into Equation (S26), ΔT = 1.19 × 10^{-8} °C is obtained. Thus, the temperature rise due to the viscous dissipation of magnetophoresis induced convection is extremely small to be noticeable.

Supplementary Information S13 – *Dye-Free Version of Figure 12*

Figure S5 illustrates the dye-free version of magnetophoresis experiments conducted by using magnets of different size (Magnet S and Magnet B).

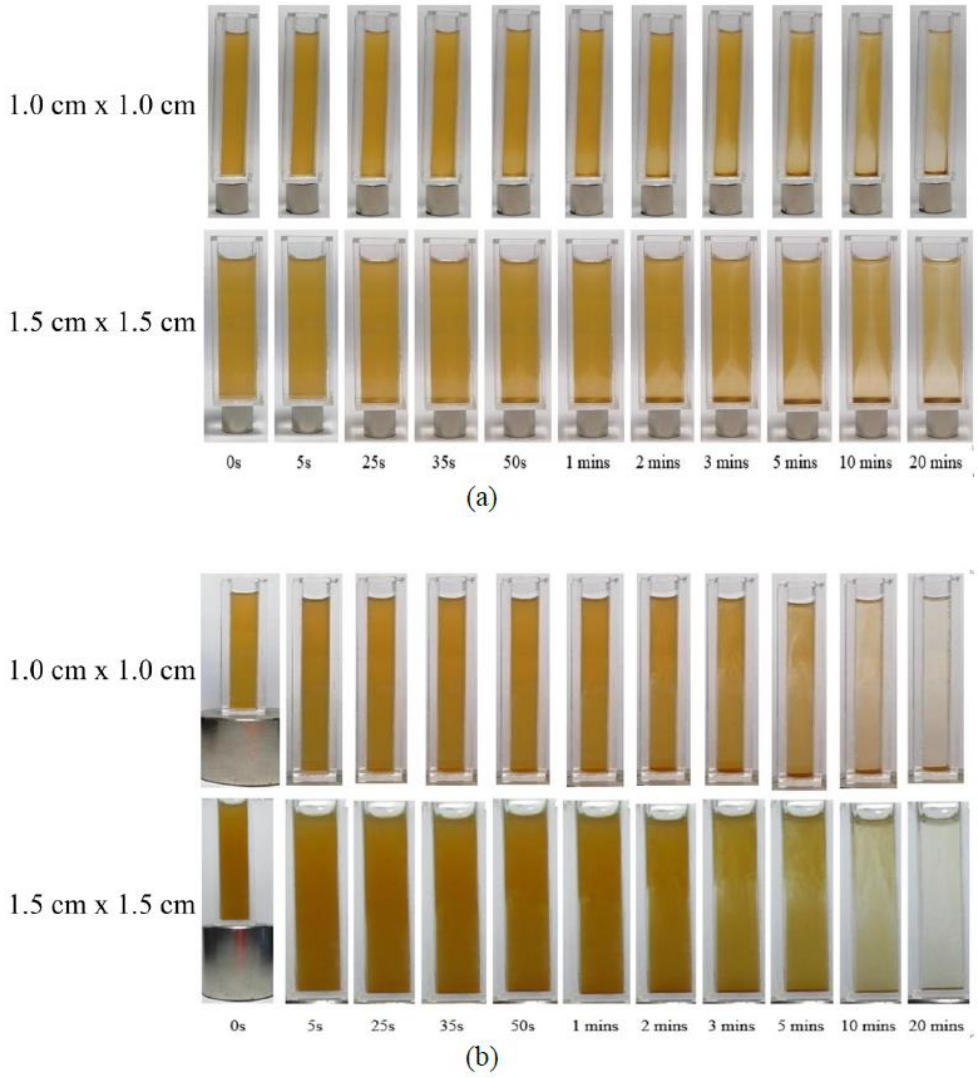

Figure S5. Time lapse images for MNP solution (dye-free version) filled in cuvettes of with base dimension of 1.0 cm × 1.0 cm and 1.5 cm × 1.5 cm, upon exposure to magnetic field generated by (a) Magnet S and (b) Magnet B, for duration of 20 minutes.

Throughout magnetophoresis experiments, MNP solutions consistently displayed uniform concentration when Magnet B is used, which implies there is a strong convective current in the MNP solution that is responsible for agitation and mixing (Figure S5(b)). On the

other hand, when smaller Magnet S was employed, the non-uniform distribution of MNPs within the solution is apparent (Figure S5(b)). Hence, it can be concluded that the induced convection is not sufficiently immense to continuously distribute MNPs throughout the solution under magnetic field create by Magnet S. This is because the magnetic field imposed by Magnet S decays very rapidly with respect to the distance from the magnet. In fact, this observation is consistent with the argument stated in Subsection 4.2.3 of the main article.

REFERENCES

[1] S.P. Yeap, A.L. Ahmad, B.S. Ooi, J. Lim, Electrosteric stabilization and its role in cooperative magnetophoresis of colloidal magnetic nanoparticles, Langmuir 28 (2012) 14878–14891. https://doi.org/10.1021/la303169g.

[2] M. Arias, E. López, A. Nuñez, D. Rubinos, B. Soto, M.T. Barral, F. Díaz-Fierros, Adsorption of Methylene Blue by Red Mud, An Oxide- Rich Byproduct of Bauxite Refining, in: J. Berthelin, P.M. Huang, J.-M. Bollag, F. Andreux (Eds.), Effect of Mineral-Organic-Microorganism Interactions on Soil and Freshwater Environments, Springer US, Boston, MA, 1999: pp. 361–365. https://doi.org/10.1007/978-1-4615-4683-2_39.

[3] R.B. Bird, W.E. Stewart, E.N. Lightfoot, Transport Phenomena, Wiley, 2001.

[4] S.S. Leong, Z. Ahmad, J.K. Lim, Magnetophoresis of superparamagnetic nanoparticles at low field gradient: Hydrodynamic effect, Soft Matter 11 (2015) 6968–6980. https://doi.org/10.1039/c5sm01422k.

[5] S.A. Khashan, E. Elnajjar, Y. Haik, CFD simulation of the magnetophoretic separation in a microchannel, J Magn Magn Mater 323 (2011) 2960–2967. https://doi.org/10.1016/j.jmmm.2011.06.001.

[6] J.S. Andreu, J. Camacho, J. Faraudo, M. Benelmekki, C. Rebollo, L.M. Martínez, Simple analytical model for the magnetophoretic separation of superparamagnetic dispersions in a uniform magnetic gradient, Phys Rev E Stat Nonlin Soft Matter Phys 84 (2011) 1–8. https://doi.org/10.1103/PhysRevE.84.021402.

[7] G.P. Hatch, R.E. Stelter, Magnetic design considerations for devices and particles used for biological high-gradient magnetic separation (HGMS) systems, J Magn Magn Mater 225 (2001) 262–276. https://doi.org/10.1016/S0304-8853(00)01250-6.

[8] M.A. Day, The no-slip condition of fluid dynamics, Erkenntnis 33 (1990) 285–296. https://doi.org/10.1007/BF00717588.

[9] S.S. Leong, Z. Ahmad, J. Camacho, J. Faraudo, J.K. Lim, Kinetics of Low Field Gradient Magnetophoresis in the Presence of Magnetically Induced Convection, Journal of Physical Chemistry C 121 (2017) 5389–5407. https://doi.org/10.1021/acs.jpcc.6b13090.

[10] G. de Las Cuevas, J. Faraudo, J. Camacho, Low-gradient magnetophoresis through field-induced reversible aggregation, Journal of Physical Chemistry C 112 (2008) 945–950. https://doi.org/10.1021/jp0755286.

[11] S.P. Yeap, S.S. Leong, A.L. Ahmad, B.S. Ooi, J. Lim, On size fractionation of iron oxide nanoclusters by low magnetic field gradient, Journal of Physical Chemistry C 118 (2014) 24042–24054. https://doi.org/10.1021/jp504808v.

[12] J.S. Andreu, J. Camacho, J. Faraudo, Aggregation of superparamagnetic colloids in magnetic fields: the quest for the equilibrium state, Soft Matter 7 (2011) 2336–2339. https://doi.org/10.1039/C0SM01424A.

[13] J. Faraudo, J.S. Andreu, J. Camacho, Understanding diluted dispersions of superparamagnetic particles under strong magnetic fields: A review of concepts, theory and simulations, Soft Matter 9 (2013) 6654–6664. https://doi.org/10.1039/c3sm00132f.